Gold nanoparticles for cancer detection and treatment: The role of adhesion

Y. Oni,[1,2] K. Hao,[3] S. Dozie-Nwachukwu,[4,5] J. D. Obayemi,[4] O. S. Odusanya,[4,5] N. Anuku,[2,6] and W. O. Soboyejo[1,2,4]
[1]*Princeton Institute for Science and Technology of Materials (PRISM), Princeton University, 70 Prospect Street, Princeton, New Jersey 08544, USA*
[2]*Department of Mechanical and Aerospace Engineering, Princeton University, Princeton, New Jersey 08544, USA*
[3]*Department of Civil and Environmental Engineering, Massachusetts Institute of Technology, Cambridge, Massachusetts 02139, USA*
[4]*African University of Science and Technology (AUST), Kilometer 10, Airport Road, Abuja, Federal Capital Territory, Nigeria*
[5]*Sheda Science and Technology Complex (SHESTCO), Gwagwalada, Abuja, Federal Capital Territory, Nigeria*
[6]*Department of Chemistry and Chemical Technology, Bronx Community College, New York, New York 10453, USA*

(Received 8 September 2013; accepted 1 January 2014; published online 26 February 2014)

This paper presents the results of an experimental study of the effects of adhesion between gold nanoparticles and surfaces that are relevant to the potential applications in cancer detection and treatment. Adhesion is measured using a dip coating/atomic force microscopy (DC/AFM) technique. The adhesion forces are obtained for dip-coated gold nanoparticles that interact with peptide or antibody-based molecular recognition units (MRUs) that attach specifically to breast cancer cells. They include MRUs that attach specifically to receptors on breast cancer cells. Adhesion forces between anti-cancer drugs such as paclitaxel, and the constituents of MRU-conjugated Au nanoparticle clusters, are measured using force microscopy techniques. The implications of the results are then discussed for the design of robust gold nanoparticle clusters and for potential applications in localized drug delivery and hyperthermia. © *2014 AIP Publishing LLC*. [http://dx.doi.org/10.1063/1.4863541]

I. INTRODUCTION

Cancer is currently the second leading cause of death in the world.[1] In most cases, the major challenge is the detection of cancer before metastasis.[1,2] Hence, the diagnosis is often too late to administer the current treatments that are available.[3,4] Consequently, more than 550 000 Americans and more than 7.5×10^6 worldwide die of cancer each year.[5] Furthermore, for the patients that undergo bulk systemic cancer treatment, the treatment is often painful, with significant short and long term side effects arising from common treatment methods that include: chemotherapy, radiotherapy, hyperthermia, and surgery.[3,4]

In an effort to reduce the potential side effects of bulk systemic cancer treatment, our previous work[6] explored the potential of an implantable anti-cancer treatment device that can locally deliver drugs and heat to the site of a tumor. Such a device can be used, following surgery to remove cancer tissue, to treat cancer by the localized chemotherapy and hyperthermia. The combination of heat and drug was selected because of the potential of engineering synergy through the combined use of localized chemotherapy and hyperthermia.[7]

However, the above device requires surgery for its insertion into the body. Furthermore, it may not treat metastatic cells that have escaped into the blood stream and other organs. There is, therefore, a need for novel approaches for the detection and treatment of cancer cells before and after metastases.[1] This has stimulated our recent efforts to use nanoparticles to facilitate the early detection and treatment of cancer.[8–11] The nanoparticles can be injected into the blood stream, where they can also diffuse through the capillaries and pores, until they reach receptors on cancer cells that can bind specifically to MRUs (such as antibodies and peptides) that are attached to them.[8]

Upon attachment, the nanoparticles can be used to facilitate the imaging[8–11] and treatment[8–11] of cancer. For example, magnetic nanoparticles may be used to facilitate the magnetic resonance imaging (MRI) of cancer cells/tissue, while gold nanoparticles may be used to enhance laser therapy through interactions that occur between gold nanoparticles and laser beams.[8] Similarly, anti-cancer drugs that are tethered to gold nanoparticles may be used to treat targeted cancer cells/tissue and metastatic cancer cells in the blood stream.[8,11] Designer nanoparticles, therefore, have the potential for localized detection and treatment of cancer.

Gold nanoparticles are particularly attractive in cancer treatment because of their strong absorption of light in the visible and near-infra red (NIR) electromagnetic regions. This optical absorption is strongly dependent on the shape and size of the gold nanoparticle.[8] Furthermore, it has been shown that the cell uptake of spherical gold nanoparticles is dependent on their size, with 50 nm being the optimal diameter.[12] Also, because smaller nanoparticles are expected to have a better chance of passing through tumor vasculature, they can attach to tumor tissue and then pass through the body prior to egestion and excretion. This prevents their long

term accumulation in the body, while providing the basis for cancer detection and treatment during their attachment to specific cancer cells.

Since the interactions between nanoparticles and cancer cells can provide a basis for cancer detection and treatment, significant efforts have been made to design gold nanoclusters that can improve our ability to detect and treat cancer.[8,11,13–21] In general, such nanoclusters consist of:

- an imaging core, such as gold that can undergo plasmon resonance under illumination with a laser;
- encapsulated anti-cancer drugs, such as paclitaxel;
- molecular recognition units, such as antibodies and peptides that bind specifically to receptors on cancer cells, ligand chemistry, and protective coatings that limit the interaction of the nanoparticles with surrounding tissue and blood during transport to target organs (Figure 1).

During transport in the body, the nanoclusters are subjected to hydrodynamic and shear forces that can cause them to fragment into smaller pieces. They must, therefore, be bound by significant adhesive and cohesive forces that cannot be overcome by the forces encountered during nanoparticle transport in the body. There is, therefore, a need to quantify the adhesion forces between the constituents of nanoclusters that are relevant to cancer detection and treatment. This can be done using Force Microscopy during Atomic Force Microscopy (AFM).[22–24] This is a technique that can be used to study bi-material pairs[25] that simulate pair-wise interactions between interacting nanoparticles.[26] It is the basis for force spectroscopy and the measurement of nano/molecular scale adhesion.[27,28]

This paper presents the results of an experimental study of the adhesion between the constituents of gold nanoclusters that are relevant to cancer detection and treatment. In the case of cancer detection, the adhesive interactions between gold nanoparticles and molecular recognition units (such as luteinizing hormone releasing hormone and a breast specific antibody) are measured using force microscopy. The adhesion between gold nanoparticles and paclitaxel (a anti-cancer drug) is also measured along with the effects of thiols that are often used to improve the adhesion between gold and a number of organic materials.[29] The implications of the results are then discussed for the development of gold nanoclusters for future applications in cancer detection and treatment.

II. THEORY

The force microscopy method involves bringing AFM tips close enough for adhesive interactions to occur (Figure 2(a)). This ultimately causes them to jump into contact (Figure 2(b)). The tips then undergo elasticity as they are displaced further in the same direction (Figure 2(c)). Upon their retraction, the displacements are reversed, as the loads are reduced to zero (Figure 2(d)). However, the tips do not detach at zero load, due to the effects of adhesion. Consequently, the retraction has to be continued until the adhesive interactions are overcome by the applied forces. This results in the pull-off of the AFM tips from the substrates (Figure 2(e)). The resulting pull-off force, F, is a measure of the adhesion. It is given by Hooke's law

$$F = k\delta, \tag{1}$$

where k is the stiffness of the AFM cantilever and δ is the displacement of the AFM tip at the onset of pull-off (represented as the length, EA in Figure 2(a)). Measurements of such pull-off forces have been applied in biology.[30–33] They have been shown to be sufficient to detect the differences between breast cancer cells and normal breast cells in recent work by Meng *et al.*,[25] who studied the adhesive interactions between the breast specific EphA2 antibodies and receptors on breast cancer or normal breast cells. Meng *et al.*[25] also studied the adhesion between luteinizing hormone releasing hormone (LHRH) peptides and their receptors on breast cancer and normal breast cells. Their results show that the pull-off forces associated with breast cancer cells and LHRH/EphA2, which are over-expressed in breast cancer cells,[34,35] are about five times the adhesion to normal breast cells.[25]

It is important to note here that although the above results suggest that force microscopy can be used to measure the adhesive forces between the constituents of nanoclusters, there have been no prior efforts to use force microscopy to measure the adhesion between gold nanoparticles and the constituents of nanoclusters that are being designed for the specific detection and treatment of cancer via localized

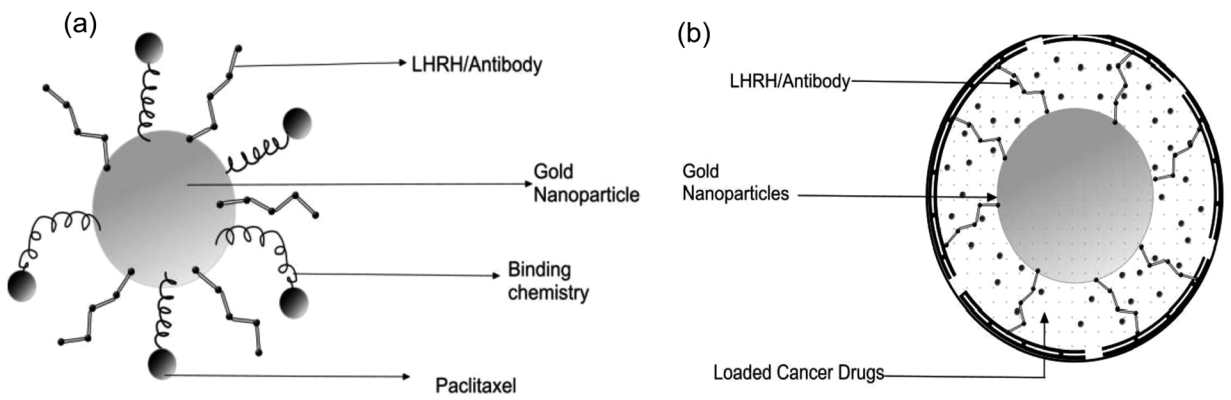

FIG. 1. Possible schematics of a nanoparticle-based drug delivery/detection system.

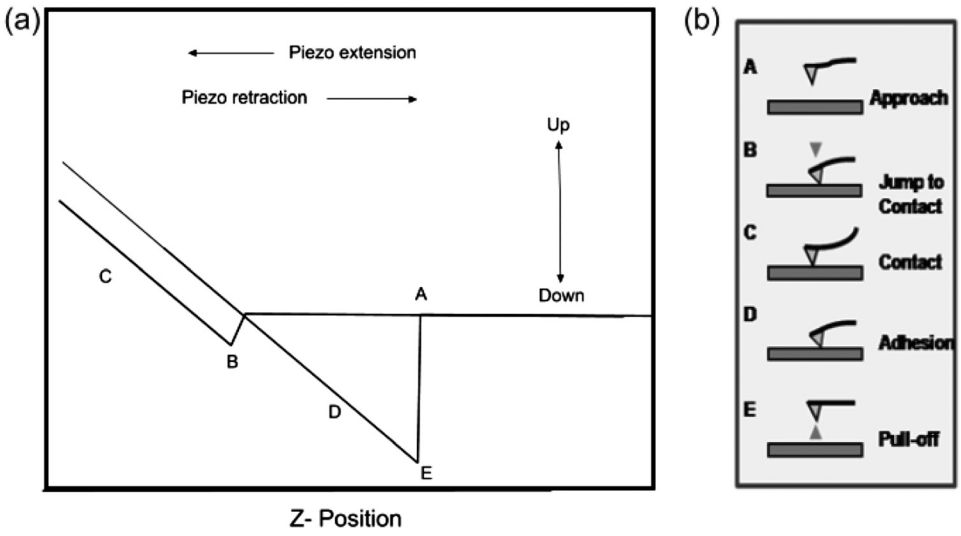

FIG. 2. Schematic of an atomic force microscope force-displacement behavior: (a) Load-displacement plot, (b) Tip/Surface Interaction. In one cycle, tip approaches the surface of the substrate (A), jumps to contact with substrate as significant van der Waals forces are felt (B), undergoes elasticity as it is displaced further in the same direction (C), displacements are reversed upon retraction as loads reduce to zero (D), tip does not detach at zero load due to the effects of adhesion until sufficient force is applied to pull the tip off the surface (E).

chemotherapy and hyperthermia. This will be explored in this study using a model nanocomposite system (Figure 1) that can deliver the anti-cancer drug, paclitaxel, while providing the basis for thermo-chemotherapy, by localized hyperthermia via plasmon resonance with optically tunable gold nanoparticle cores.

III. MATERIALS AND METHODS

A. Materials

The gold nanoparticles were purchased from Nanopartz Inc. (Loveland, CO), while the uncoated AFM tips were procured from Veeco (Memphis, TN). Paclitaxel was obtained from Parenta Pharmaceuticals (West Colombia, SC), while LHRH was purchased from Thermo Scientific (Waltham, MA). The Breast Specific Antibody (BSA) and thiols were obtained from Sigma-Aldrich (St. Louis, MO).

B. AFM experiments

1. AFM tip and substrate coating/characterization

A simple dip-coating method[25] was used to coat the AFM tips. The bare AFM tips were dip-coated with either gold nanoparticles, LHRH or BSA. This was done by immersing them into their respective solutions for about 10 s to maximize the AFM tip surface contact with the solution. The tips were then air-dried for less than a minute, after which they were dipped for a second time, again for 10 s. This procedure was repeated 3–5 times to complete the coating process. The nanoparticle concentrations in solution ranged from 22 to 46 ppm. These were used in the as-received condition. Similarly, the BSA, thiols and LHRH solutions were used, as provided by the vendors, at a concentration of 0.5 mg/ml.

Subsequently, the coated AFM tips were air-dried for a minimum of 24 h. They were then observed under a scanning electron microscope. The paclitaxel, LHRH, and BSA substrates were prepared by spreading each of the solutions on glass sheets to form thin layers. These were then allowed to dry in air for a minimum of 24 h. The surface morphologies of the coated substrates and the uncoated glass substrates (control surfaces)[36] were then characterized using a Dimension 3100 Atomic Force Microscope (AFM) that was operated in the tapping mode (Dimension 3100, Bruker Instruments, Woodbury, NY, USA).

In order to confirm that the AFM tip samples were coated with gold nanoparticles, the coated and bare tips were imaged under a Phillips Model FEI XL30 field emission gun scanning electron microscope (SEM) (Phillips Electronics N.V., Eindhoven, The Netherlands). The images were obtained using secondary electron imaging. The images of the coated AFM tips were obtained before and after the AFM experiments. In this way, possible detachment or delamination of the coatings was observed on the coated AFM tips.

Hence, since pull-off forces were only accepted for cases in which the coatings were still present after the pull-off experiments, the measured pull-off forces were confirmed to be due to the intended bi-material pairs. The spring constants of the coated and uncoated tips were measured using the thermal tune method.[37,38] This was measured because the actual spring constants are needed to obtain the true adhesion forces from Eq. (1). This also accounts for batch-to-batch variations in the spring constants, as well as the effects of coatings on the cantilever stiffness.[25,36] The pull-off measurements were obtained under ambient conditions (room temperature of 22–23 °C and a relative humidity of 40–45%).

2. AFM force-displacement measurements

The interactions between the gold nanoparticle-coated AFM tips and the cell substrates or between the components of the drug delivery systems were measured using a Multimode Dimension DI Nanoscope IIIa Atomic Force Microscope (Bruker Instruments, Woodbury, NY, USA). The measurements were obtained under ambient conditions and relative humidity (40–45%). The photodetector sensitivity was calibrated on a stiff quartz surface before force microscopy measurements.[39] The Veeco probes were made from uncoated phosphorus (n)-doped silicon. They have a tip radius of curvature of 30 nm. For each pair of interactions,

TABLE I. Substrates and coated tips used in AFM study.

Coating on tip	Substrate
Gold	Taxol (Paclitaxel)
Gold	Taxol (Paclitaxel)
Gold	Antibody
Antibody	Taxol (Paclitaxel)
LHRH	Taxol (Paclitaxel)

150 adhesion measurements were obtained from 3 AFM tips with 50 measurements obtained for each tip at 5 different positions on the substrate.

Table I shows the different pairs used.

IV. RESULTS AND DISCUSSION

A. AFM tip and substrate characterization

Back-scattered SEM images of the uncoated and dip-coated AFM tips are presented in Figures 3(a)–3(g). The images show tips before and after the AFM adhesion measurements. A typical uncoated AFM tip is shown in Figure 3(a). This shows that the bare tip is evenly smooth along the corners and surfaces of the tip. However, in the case of the coated tips, corners and apexes are covered with coatings that disrupt the smoothness of the surfaces.

Typical AFM images of the dip-coated AFM tips are presented in Figures 3(b)–3(f). These show the surface morphologies of AFM tips that are coated with nanoscale layers of gold (Figure 3(b)), LHRH (Figure 3(c)), EphA2 breast specific antibody (Figure 3(d)). Furthermore, no evidence of coating delamination was observed on the surfaces of the coated AFM tips that were used in the pull-off experiments. Hence, the measured pull-off forces are due to interactions between the coated AFM tips and the substrates.

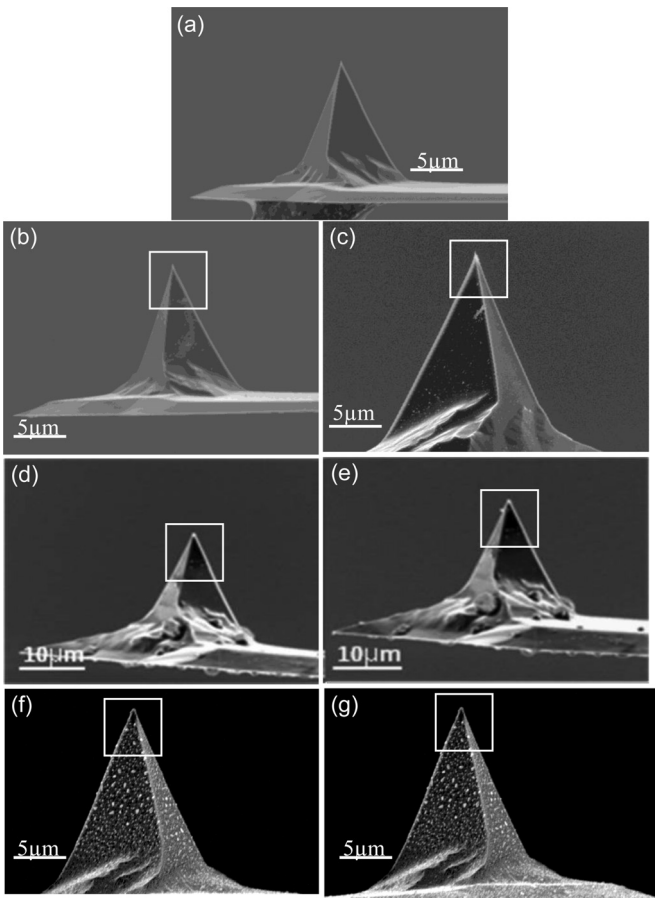

FIG. 3. Sample SEM Images of the AFM tips: (a) Bare AFM tip; (b) Gold nanoparticles-coated AFM tip before adhesion measurement; (c) Gold nanoparticles-coated AFM tip after adhesion measurement; (d) LHRH-coated AFM tip before adhesion measurement; (e) LHRH-coated AFM tip after adhesion measurement; (f) BSA-coated AFM tip before adhesion measurement; (g) BSA-coated AFM tip after adhesion measurement. Boxes show coating on apex tip and side edges.

B. Adhesion forces

Figure 4 shows a typical force-displacement plot for the adhesion between gold nanoparticles and LHRH. This plot has characteristics similar to the idealization presented in Figure 2. By multiplying the pull-off deflections with the tip stiffness shown in Table II, the pull-off forces were obtained. There were no measurable forces for the control samples.

The adhesive force interactions between the different components of the designer drug delivery system (shown in Figure 1) are presented in Figure 5. The adhesion forces between the gold nanoparticles and LHRH and between gold nanoparticles and BSA are comparable and stronger than those obtained for paclitaxel-gold, paclitaxel-antibody or paclitaxel-LHRH complexes.

The weakest adhesive interactions within the drug nanocomposite systems (Figure 5) are with the drug (paclitaxel). These interactions result in pull-off forces of about 10 nN, compared to those without the drug ($F \sim 58$ nN). This suggests that the robustness of such systems will depend highly on the drug-component interactions.

These above adhesion forces are generally related to Van der Waal's forces, with relatively large and short range interactions between the different components. Also, it can be observed that similar adhesion forces were obtained for the LHRH and BSA coated tips when measured against the

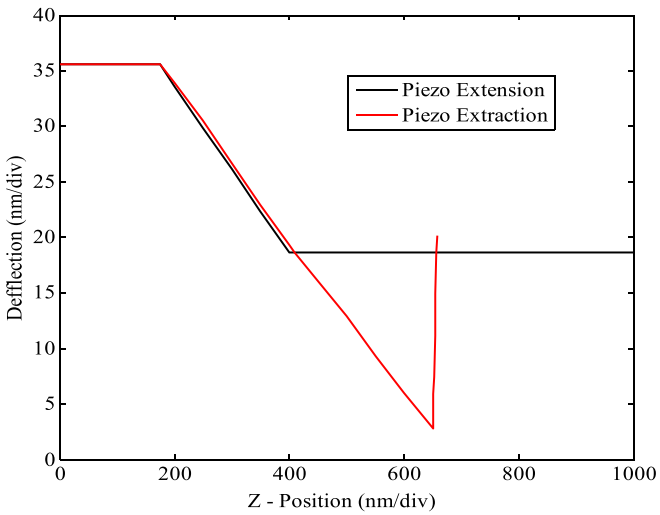

FIG. 4. Typical AFM force-displacement behavior for coated tips on substrates.

TABLE II. Spring constants of the bare and coated tips.

LHRH-coated tip	0.71 ± 0.11
Gold-coated tip	0.48 ± 0.21
Antibody-coated tip	1.02 ± 0.32

same substrate (~60 nN against gold and ~10 nN against paclitaxel). This may be due to the amino acid sequence present in the peptide and polypeptide structures in the LHRH and BSA, respectively. The overall adhesion forces would, therefore, depend on the charge distributions and positions of the amino acid residues in the peptide and polypeptide structures of the LHRH and BSA structures.

The AFM force microscopy results (Figure 5) also show that gold nanoparticles are strongly attracted to biological compounds. The pull-off forces for gold-LHRH and gold-AB pairs are 60 ± 3 nN and 57 ± 3 nN, respectively. These forces are presented in Table III.

These are far greater than those between gold and paclitaxel, which is 12 ± 0.6 nN. In contrast, there are weak adhesive interactions between paclitaxel and the molecular recognition units, LHRH and Antibody. The adhesive forces obtained for these interactions are 10 ± 1 nN and 9 ± 1 nN, respectively. The results are shown in Table IV.

The adhesion forces between taxol and gold, as well as taxol and thiol are generally less than the other interactions within the nanocomposite drug delivery system. Hence, the current results show that the drug is the weak link in the nanocomposite system. Careful nanocluster engineering must, therefore, be carried out to prevent the inadvertent release of the drug, paclitaxel, before it is delivered to the tumor sites for controlled release and the treatment of cancer cells/tumor tissue.

Furthermore, the results show that the presence of thiols plays an important role in the overall robustness of the system. Figures 6–8 reflect increased adhesion forces, when compared with those with gold. In Figure 6, the thiol-antibody couple has an adhesion force of 320 ± 40 nN, which is about three times the adhesion force between gold and the breast specific antibody. These results are summarized in Table V.

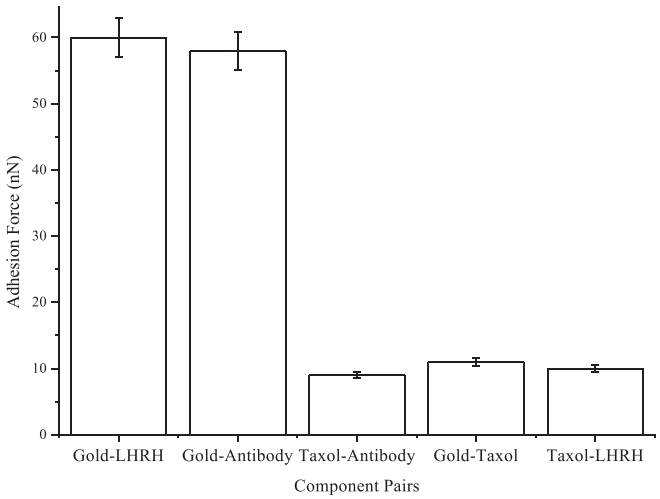

FIG. 5. Adhesion interactions of components in a drug delivery system.

TABLE III. Comparison of adhesion interactions for LHRH with and without thiols.

Component pairs	Average adhesion force (nN)
Gold-LHRH	60 ± 3
Gold-Antibody	57 ± 3
Gold-Thiol	100 ± 5
LHRH-Thiol	200 ± 10

TABLE IV. Comparison of adhesion interactions for paclitaxel (taxol) with antibody, gold or LHRH.

Component pairs	Average adhesion force (nN)
Taxol-thiol antibody	9 ± 1
Taxol-gold	12 ± 0.6
Taxol-LHRH	10 ± 1

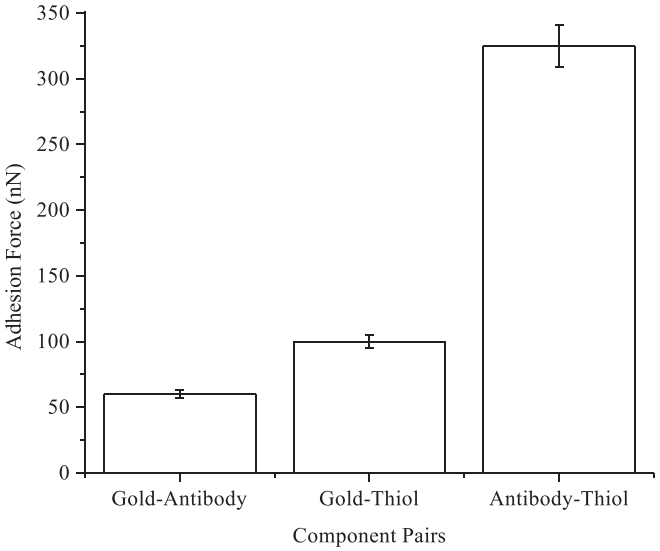

FIG. 6. Comparison of adhesion interactions for Gold with and without thiols.

TABLE V. Comparison of adhesion interactions for Gold with and without thiols.

Component pairs	Average adhesion force (nN)
Gold-antibody	60 ± 3
Gold-thiol	100 ± 5
Antibody-thiol	320 ± 40

Also, the adhesion force between thiol and gold is found to be almost double that between the gold and the BSA. These results clearly indicate a significant increase in the adhesive interactions when thiol is introduced between the gold and BSA. The increased adhesion forces between gold and thiol can be attributed to covalent bonds. Gold is known to form stable complexes with ligands which have "soft" or polarizable electron donating atoms such as phosphorus or sulfur.[40] Similarly, the stronger adhesive forces between BSA and thiol may be attributed to amine-thiol interactions.

Similar results were obtained for LHRH interactions. These resulted in a three-fold increase in the adhesion forces of gold-thiol structures, when compared with those of uncoated gold structures (Figure 7). Furthermore, the adhesion forces between gold and paclitaxel are about six times greater when thiols are present (Figure 8). The current results, therefore, confirm that thiols can improve the robustness of gold nanoparticle clusters, as is expected from prior work reported in the literature.[41,42] The current results are also presented in Table VI.

The above results suggest that, with the exception of thiol-taxol interactions, the interactions between thiol and the other chemical species (LHRH, EphA2 and gold) generally result in increased adhesion. These results are shown in Table VII.

The observed increase in adhesion forces (in the presence of thiols) is attributed to the effects of secondary bonds (Van der Waals forces or hydrogen bonds). Furthermore, the statistical variations in the measured adhesion forces seem to be less in the cases where the number of molecular species on the AFM tips are fewer. However, in cases with increased numbers of available molecular species on the AFM tips (taxol and LHRH), the variabilities in the measured adhesion forces may depend on the coverage of the AFM tips and the orientations of the molecules on the AFM tips and the substrates. Further work is clearly needed to explore the effects of molecular orientation and AFM tip coverage on the measured adhesion forces. These are clearly some of the challenges for future work.

The reasons for the variations in error ranges in the adhesion force measurements are not fully understood at the moment. We also note that the adhesive interactions between relatively large antibodies and gold nanoparticles result in smaller statistical variations, while those between organic structures with many possible sites of interactions result in larger variations in adhesive force.

Finally in this section, Figure 9 provides a comparison of the forces obtained for the different component pairs with

TABLE VI. Comparison of adhesion interactions for LHRH with and without thiols.

Component pairs	Average adhesion force (nN)
Gold-LHRH	60 ± 3
Gold-thiol	100 ± 5
LHRH-thiol	200 ± 10

TABLE VII. Comparison of adhesion interactions of the nanocomposite components with thiols.

Component pairs	Average adhesion force (nN)
Gold-thiol	100 ± 5
Antibody-thiol	320 ± 6
LHRH-thiol	200 ± 10
Taxol-thiol	65 ± 3

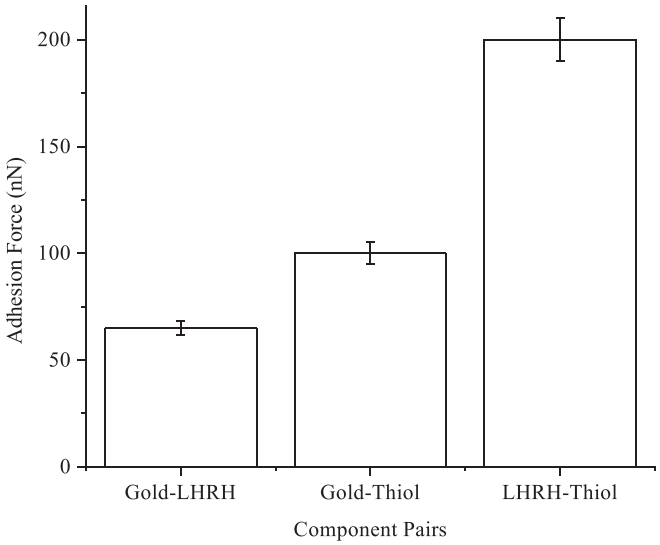

FIG. 7. Comparison of adhesion interactions for LHRH with and without thiols.

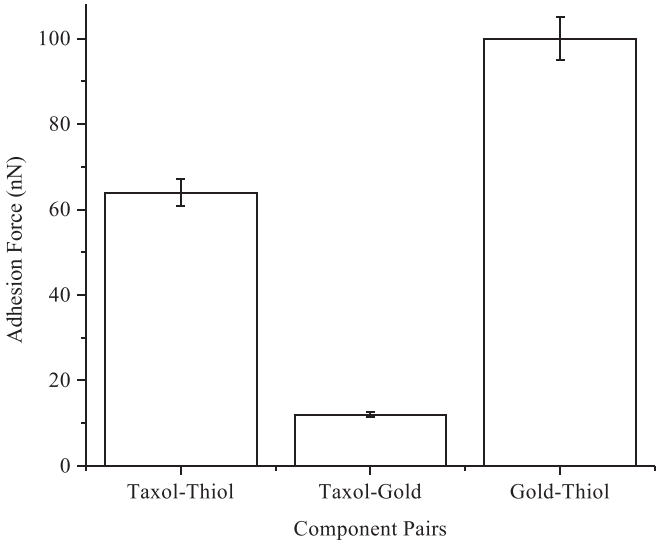

FIG. 8. Comparison of adhesion interactions for Paclitaxel (taxol) with and without thiols.

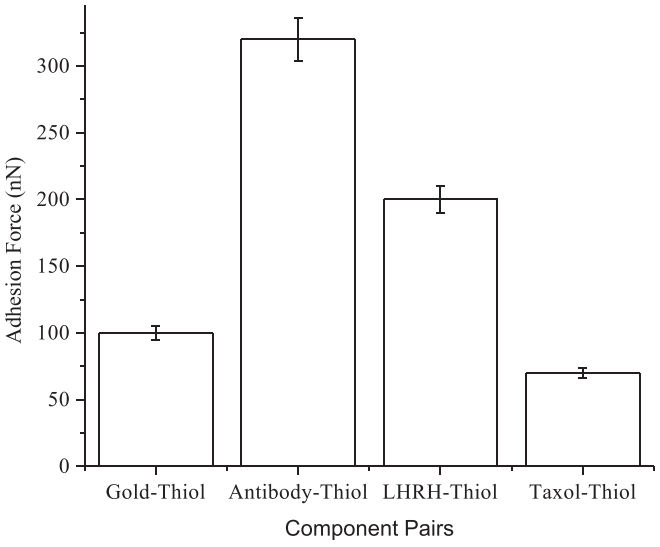

FIG. 9. Comparison of adhesion interactions of the nanocomposite components with thiols.

thiols. As reported previously,[43] proteins have the strongest affinity to thiols due to the possible disulfide intermolecular interactions.

Covalent bonds between gold and thiols[40] may be responsible for these strong adhesive interactions. Furthermore, the paclitaxel-thiol bi-material pair results in the smallest pull-off forces, suggesting the presence weak Van der Waal's interactions.

V. IMPLICATIONS

The implications of the current work are quite significant. They suggest that nanoparticles, peptides and antibodies can be coated on micro-cantilever tips and used to measure adhesion interactions that are relevant to drug delivery systems. Hence, the pairwise adhesive interactions between the drug components can be measured using force microscopy techniques. However, there is a need for further work to explore the extent to which the AFM adhesion measurements may vary due to interactions with liquids and different solvents that are relevant to *in-vitro* and *in-vivo* environments. *In-vitro* and *in-vivo* studies are also needed to understand the level to which the AFM adhesion measurements can be related to nanoparticle-drug component interactions and binding under experimental and clinical conditions. These are clearly some of the challenges for future work.

Based on the sizes of the rounded AFM tips with tip radii of about 30 nm, we estimate a total hemi-spherical volume of about 5656 nm^2 is available for the adhesive interactions with the substrates. Hence, in the case of the EphA2 antibodies, if we estimate the surface areas of the molecules to be approximately 1000 nm^2, then we would expect to have about 5.7 molecules interacting with the substrates. Consequently, partial coverage of the tip rounded AFM tips should result in about 3–5 molecules per rounded AFM tip. In the case of the smaller LHRH peptides, with surface areas of about 36 nm^2, about 157 LHRH peptides can be attached to the rounded AFM tip, if it is fully covered. Similarly, the interactions with the taxol drug molecule with a surface area of 100 nm^2 could result in about 57 taxol molecules on the rounded AFM tip.

Furthermore, it is also clear that the adhesion methods that were used in this study can be used to screen the effectiveness of potential binding chemistry and coated nanoparticle targets before conducting expensive *in-vitro* and *in-vivo* studies that are needed for clinical use. However, the relatively weak bonds between the anti-cancer drugs (paclitaxel) suggest that nanocluster fragmentation may occur during transportation in the bloodstream to the target organs. Since such fragmentation may result in premature drug release from the nanoparticle clusters (before they reach the intended tumor tissue/target organs), there is a need for further experimental and computational work to study the resistance of the nanoparticle clusters to fragmentation under *in-vitro* and *in-vivo* conditions. Nevertheless, the results of the current study show clearly that thiols improve the adhesion between the constituents of nanoclusters that are relevant to early cancer detection and the localized treatment of cancer via hyperthermia and localized drug release.

VI. CONCLUSIONS

This paper presents the results of an experimental study of the adhesion forces between components of a model generic drug delivery/system that includes gold nanoparticles, paclitaxel, thiols, LHRH and as breast-specific antibody, BSA. The results confirm that the robustness of such systems depends on the adhesion to paclitaxel, which is the weak link. In such cases, it is important to design nanoparticle clusters in which adhesion to the drug is increased to prevent premature release. The results suggest that the force microscopy technique can be used to rank the adhesion between different species in drug nanocomposites that are being developed to treat breast cancer and other forms of cancer. They also show that the presence of thiols can significantly increase the adhesive forces between gold and the molecular recognition units or the drugs in these systems. Furthermore, the current work provides a tool for fast screening of potential binding chemistry for ligand conjugated nanoparticles that can also be used for cancer detection and treatment. Further work is clearly needed to measure the adhesion forces in biological environments and clinical settings.

ACKNOWLEDGMENTS

This work was supported by the National Science Foundation (Grant No DMR 0231418), the Princeton Grand Challenges Program, the World Bank STEP B Program, the World Bank African Centers of Excellence Program and the African Development Bank. The authors are grateful to these agencies for their financial support and encouragement. We would also like to extend our appreciation to Wali Akande, Rose Ndong and Tiffany Tong for their assistance in the AFM measurements.

[1]L. A. Nagahara, M. Ferrari, and P. Grodzinski, MRS Bull. **34**, 406–414 (2009).
[2]P. Grodzinski, M. Silver, and L. K. Molnar, Expert Rev. Mol. Diagn. **6**, 307–318 (2006).
[3]D. Irvine, L. Vincent, J. E. Graydon, N. Bubela, and L. Thompson, Cancer Nursing **17**(5), 367–378 (1994).
[4]*Le Cancer Dans le Monde* edited by B. W. Stewart and P. Kleihues (C.I.d.R.s.I.C. (CIRC), IARC Press, Lyon, 2005).
[5]A. Jemal, M. J. Thun, L. A. G. Ries, H. L. Howe, H. K. Weir, M. M. Center, E. Ward, X. C. Wu, C. Eheman, A. Anderson, U. A. Ajani, B. Kohler, and B. K. Edwards, J. Nat. Cancer Inst. **100**, 1672–1694 (2008).
[6]Y. Oni, C. Theriault, A. V. Hoek, and W. O. Soboyejo, Mater. Sci. Eng. C **31**(2), 67–76 (2011).
[7]R. Kurzrock and M. Markman, *Targeted Cancer Therapy* (Humana Press, Clifton, 2008).
[8]M. P. Melancon, W. Lu, and C. Li, MRS Bull. **34**, 415–421 (2009).
[9]M. Ferrari, Nat. Rev. Cancer **5**, 161–171 (2005).
[10]M. V. Yezhelyev, X. Gao, Y. Xing, A. Al-Hajj, and O'. R. M. Nie Shuming, Lancet Onco **7**(8), 657–667 (2006)..
[11]R. G. Ramachandra, S. Mahaveer, and B. D. Ross, Clini. Can. Res. **12**, 6677 (2006).
[12]D. L. Thorek and A. Tsourkas, Biomaterials **29**(26), 3583–3590 (2008).
[13]A. H. Lu, E. L. Salabas, and F. Schuth, Angew Chem. Int. Ed. Engl. **46**(8), 1222–1244 (2007).

[14]S. Laurent, D. Forge, M. Port, A. Roch, C. Robic, L. Vander Elst, and R. N.Muller, Chem. Rev. **108**, 2064–2110 (2008).
[15]J. Kim, S. Park, E. L. Ji, S. M. Jin, J. H. Lee, L. S. Lee, I. Yang, J. S. Kim, S. K. Kim, M. H. Cho, and T. Hyeon, Angew. Chem. Int. Ed. **45**(46),7754–7758 (2006).
[16]W. Stöber, A. Fink, and E. Bohn, J Colloid Interface Sci. **26**(1), 62–69 (1968).
[17]S. I. Stoeva, F. Huo, J. S. Lee, and C. A. Mirkin, J. Am. Chem. Soc. **127**(44), 15362–15363 (2005).
[18]V. Salgueirino-Maceira, M. A. Correa-Duarte, M. Farle, A. Lopez-Quintela, K. Sieradzki, and R. Diaz, Chem. Mater.**18**(11), 2701–2706 (2006).
[19]M. Chen, Y. N. Kim, H. M. Lee, C. Li, and S. O. Cho, Phys. Chem. C **112**, 8870–8874 (2008).
[20]H. Wang, D. W. Brandt, F. Le, P. Nordlander, and N. J. Halas, Nano. Lett. **6**(4), 827–832 (2006).
[21]L. Wang, J. Bai, Y. Li, and Y. Huang, Angew. Chem. Int. Ed. Engl. **47**(13), 2439–2442 (2008).
[22]G. Binnig, C. F. Quate, and Ch. Gerber, APS J. Phys. Rev. Lett. **56**, 930–933 (1986).
[23]R. Wiesendanger, *Scanning Probe Microscopy and Spectroscopy: Methods and Applications* (Cambridge University Press, Cambridge, 1994).
[24]S. N. Magonov and M. H. Whangbo, *Surface Analysis with STM and AFM: Experimental and Theoretical Aspects of Image Analysis* (VCH, Weinheim, 1996).
[25]J. Meng, E. Paetzell, A. Bogorad, and W. O. Soboyejo, J. Appl. Phys.**107**, 114301 (2010).
[26]C. B. Prater, P. G. Maivald, K. J. Kjoller, and M. G. Heaton, Force Spectroscopy, "See www.braker.com."
[27]P. G. Hartley, F. Grieser, P. Mulvaney, and G. W. Stevens, Langmuir **15**, 7282–7289 (1999).
[28]H. J. Butt, B. Cappella, and M. Kappl, Surf. Sci. Rep. **59**, 1–152 (2005).
[29]C. C. Berry and A. S. G. Curtis, J. Phys. D: Appl. Phys. **36**, R 198 (2003).
[30]P. Hinterdorfer, G. Schütz, F. Kienberger, and H. Schindler, Rev. Mol. Biotechnol. **82**, 25 (2001).
[31]V. Dupres, F. D. Menozzi, C. Locht, B. H. Clare, N. L. Abbott, S. Cuenot, C. Bompard, D. Raze, and Y. F. Dufrene, Nat. Methods **2**, 515–520 (2005).
[32]E. Wojcikiewicz, X. Zhang, and V. Moy, Biol. Proced. Online **6**, 1–9 (2004).
[33]F. Li, S. D. Redick, H. P. Erickson, and V. T. Moy, Biophys. J. **84**, 1252–1262 (2003).
[34]W. R. Miller, W. N. Scott, R. Morris, H. M. Fraser, and R. M. Sharpe, Nature **313**, 231–233 (1985).
[35]D. P. Zelinski, N. D. Zantek, J. C. Stewart, A. R. Irizarry, and M. S. Kinch, Cancer Res. **61**, 2301–2306 (2001).
[36]K. V. Wolf, Z. Zong, J. Meng, A. Orana, N. Rahbar, K. M. Balss, G. Papandreou, C. A. Maryanoff, and W. Soboyejo, Biomed. Mater. Res. Part A **87A**, 272–281 (2008).
[37]J. L. Hutter and J. Bechhoefer, Rev. Sci. Instrum. **64**, 1868–1873 (1993).
[38]G. A. Matei, E. J. Thoreson, J. R. Pratt, D. B. Newell, and N. A. Burnham, Rev. Sci. Instrum. **77**, 083703 (2006).
[39]B. Bhushan, *Handbook of Micro/Nanotribology* (CRC, Boca Raton, 1995).
[40]R. G. Pearson, Struct. Bonding **80**, 1–10 (1993).
[41]A. Kassam, G. Bremner, B. Clark, and B. R. Lennox, J. Am. Chem. Soc. **128**(11), 3476–3477 (2006).
[42]Z. M. Fresco and J. M. J. Frechet, J. Am. Chem. Soc. **127**(23), 8302–8303 (2005).
[43]N. Ohmura, K. Tsugita, J. I. Koizumi, and H. Saika, J. Bacteriol. **178**(19), 5776–5780 (1996).